ResearchGate

See discussions, stats, and author profiles for this publication at: https://www.researchgate.net/publication/281715488

Integrated Fault and Hazard Analysis in Downtown Houston, Texas

Article · September 2015

CITATION
1

READS
356

3 authors:

Jingqiu Huang
University of Houston
8 PUBLICATIONS **18** CITATIONS

SEE PROFILE

Don van Nieuwenhuise
University of Houston
21 PUBLICATIONS **61** CITATIONS

SEE PROFILE

Shuhab D Khan
University of Houston
121 PUBLICATIONS **1,481** CITATIONS

SEE PROFILE

Some of the authors of this publication are also working on these related projects:

Project ARCS & DARCS; Rifts & Sutures; Testing the Wilson Cycle in North America View project

Project Collision Tectonics - Pakistan View project

All content following this page was uploaded by Shuhab D Khan on 13 September 2015.

The user has requested enhancement of the downloaded file.

GCAGS JOURNAL
A Publication of the Gulf Coast Association of Geological Societies
www.gcags.org

Integrated Fault and Hazard Analysis in Downtown Houston, Texas

Jingqiu Huang, Don Van Nieuwenhuise, and Shuhab D. Khan

Department of Earth and Atmospheric Sciences, University of Houston, 312 Science and Research Bldg. 1, 4800 Calhoun Rd., Houston, Texas 77204–5007, U.S.A.

ABSTRACT

Active faults in urban areas are hazards that can cause damage to critical infrastructures. Previous works have mapped over 300 faults in Houston and surrounding areas, but many active faults remain to be found and mapped. This study locates and images faults in the highly populated medical center and university areas just south of downtown Houston. It is challenging to identify faults in densely populated urban areas so we performed an integrated geophysical survey. This study presents data from aerial light detecting and ranging (LiDAR), two-dimensional seismic profiles, and a gravity profile to map subsurface fault segments. Gravity modeling revealed faults near the Pierce Junction Salt Dome and surrounding area. The deepest fault mapped at the cross point of the two seismic profiles dips to the southeast and the measured displacement across the fault is ~20 m.

INTRODUCTION

The Houston Embayment is bounded by the Talco, Mexia and Luling fault zones that strike northeast-southwest and are extensional structures sliding toward the Gulf Coast (Ewing and Lopez, 1991). The surface fault exposures are younger toward the Gulf Coast (Fig. 1). Surface deformation caused by faults along the Texas coast between Beaumont and Victoria has been active since at least the Pleistocene and continuous through the Holocene (Engelkemeir et al., 2010; Verbeek, 1979).

Gravity driven deformation and salt movement in the northern Gulf of Mexico is responsible for the creation of numerous northeast-southwest striking normal fault systems (Diegel et al., 1995; Jackson and Galloway, 1984; Peel et al., 1995; Rowan et al., 1999; Saribudak, 2011; Worrall and Snelson, 1989; Wu et al., 1990). Around 80% of the faults in the Houston area are directly associated with salt domes (Verbeek and Clanton, 1981). Houston and its surrounding areas contain over 300 active faults (Engelkemeir and Khan, 2008). It is difficult to map all of these faults, because many do not show obvious surface expressions. Although some of the cultural footprint in Harris County aids in revealing fault traces and offsets, in other cases it can conceal their subtle displacements.

Previously a number of major faults have been recognized by field observation. Also, more subtle faults have been recognized using aerial photos in the past (Clanton and Verbeek, 1981). Two-dimensional resistivity data acquired by a dipole-dipole array was used in mapping the Willow Creek Fault (Saribudak and Van Nieuwenhuise, 2006). More recently, light detecting and ranging (LiDAR) and global positioning satellite (GPS) data have been used to map surface deformation resulting from the Hockley-Conroe Fault System, the Addicks Fault System, and the Long Point–Eureka Heights Fault System in Houston (Khan et al., 2013). The results of that study revealed up to ~56 mm/yr subsidence in northwestern Houston (Engelkemeir et al., 2010; Engelkemeir and Khan, 2008). The GPS rate from 2007–2011 shows that the south side of Houston has a higher subsidence value when compared to the north side (Khan et al., 2014). Yu et al. (2014) concluded that subsidence is only caused by sediment compaction in the top 600 m by using extensometer and GPS data. The influence of water withdrawal from aquifers on subsidence in the Houston metropolitan area has been studied (Holzer and Bluntzer, 1984; Winslow and Doyel, 1954), but the effects of salt dome deformation due to related faults have been overlooked. The Pierce Junction Salt Dome movement was previously delineated using 4D gravity measurements (Huang, 2012).

Surface deformation is the result of salt movement, faulting, and fluid withdrawal coupled with compaction. In order to understand these mechanisms further, it is necessary to quantify the influence of salt and associated faults on surface deformation. Many faults have been recognized by their surface expressions and exploration drilling activities. However, there are many additional faults that do not have an obvious surface expression. By using a novel integrated approach that combines seismic, LiDAR, and gravity data, we were able to find unknown fault segments. Some of those faults remain active today, and it is

Copyright © 2015. Gulf Coast Association of Geological Societies. All rights reserved.

Manuscript received March 31, 2015; revised manuscript received August 28, 2015; manuscript accepted August 30, 2015.

GCAGS Journal, v. 4 (2015), p. 147–154.

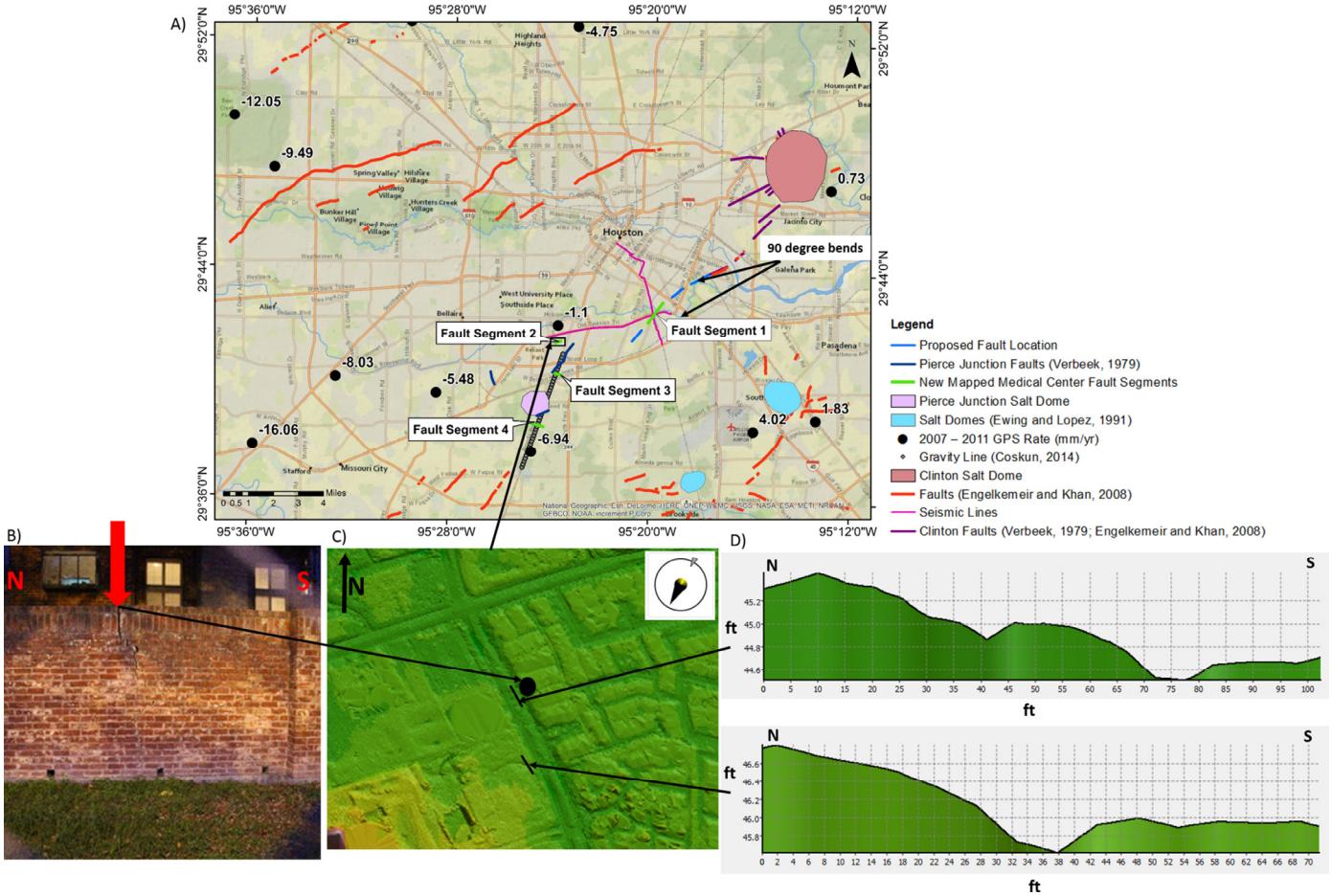

Figure 1. (A) Map showing location of study area. Major faults of the Houston area are shown as red lines, and black dots display subsidence rates measured by GPS from 2007–2011 indicating overall subsidence in and around the study area. (B) The cracks indicated by the red arrow were observed in a wall that separates a busy city street from an apartment complex. Location of the cracks is at the black dot location from hillshade map in Figure 1C. (C) Hillshade map generated from LiDAR data, an illumination altitude of 30° and azimuth of 15° were used to show two east-west trending normal fault segments in fault segment 2. Black lines show the elevation profiles across the two segments. (D) The elevation profiles along the black lines are shown in Figure 1C. The scarps have around 0.8 ft (~0.25 m) of displacement.

important to find them because of their potential impact on infrastructure. Hidden faults could cause future displacement due to fluid withdrawal.

DATASETS AND METHODS

Aerial LiDAR Hillshade

LiDAR data are publicly available in the Houston area for the years of 2001 and 2008 (TNRIS, 2015). Terrapoint LLC collected the 2001 dataset with a horizontal accuracy of ±75 cm and vertical accuracy of ±15 cm. The 2008 dataset was collected by Merrick & Company with horizontal accuracy of ±70 cm and vertical accuracy of ±9.25 cm. A number of different altitudes and azimuths were tested for the LiDAR hillshade map, and found that an altitude of 30° and azimuth of 15° illuminates the critical features (Fig. 1). The low elevation angle used (30°) highlights streets and fault scarps, whereas higher elevation angles would result in less contrast (Engelkemeir and Khan, 2008). Two anomalies in fault segment 2 have been found on the generated hillshade map (Fig. 1). Regions of interest identified in the hillshade surfaces were investigated during targeted fieldwork. Recorded observations confirmed the existence, identified the location, and provided strain information for the faults identified using the hillshade surfaces.

Visual and Field Observation

In the medical center region, shown in Figure 1, cracks were observed in a wall that separates a busy city street from an apartment complex built in 1983. The location of the cracks is situated at the one of the anomalies mapped on the hillshade map. The photograph taken in 2014 of the crack in the apartment complex wall indicates that the upthrown side is to the north. Even though fault movement is ongoing, the walls are now being rebuilt with reinforced foundations because of the potential dangers presented by the cracks. These cracks provide evidence of active faults in this area. Surface deformation was also seen on road surfaces in this area.

Examination of subsurface maps available from the Geomap Company (2015) on the top of the Vicksburg Formation in Houston show that bayous in Harris County flow either down subsurface regional dip or along subsurface regional strike. This phenomenon is seen throughout the area and indicates that in this low relief setting, regional dip has affected drainage patterns to a large extent over time. This of course is not unexpected. However, there is a significant and obvious exception to this trend in the region of fault segment 1. Here it can be observed that Brays Bayou takes two ~90° turns that are unique in their acuteness and an associated shift in flow between them that suggests the flow of the bayou turns up structural dip (Fig. 1). This exception led us

to consider that we might find a fault near these bends prior to acquiring seismic data. Its coincidence with our seismic evidence is intriguing. Consequently, we will investigate this area in the future with GPR and additional surface observations to further understand this shift in the flow pattern as well as the extent of the fault suspected by this surface expression. Especially, to confirm whether or not this is evidence of the same fault seen on the north-south seismic profile.

The seismic line reveals ~20 m of displacement with the fault dipping to the southeast. At some point displacement of the hanging-wall block presumably would have rotated into the regional dip and created a surface tilting towards the north and approximately opposite the existing regional dip. This would cause the flow to shift sharply from regional strike to being opposite the regional dip. That flow would again turn sharply in conformance with the regional strike to the east when it encountered the exposed fault scarp at the time of this shift. We will need additional data to document this fully. However, considering the patterns we see throughout Harris County, this is a very compelling explanation for the atypical flow direction and the acute bends that are out of character with the regional drainage patterns.

2D Seismic Profile

DAWSON Geophysical Company carried out field acquisition of the seismic data in the August 2013. The seismic survey includes two lines around the University of Houston main campus, oriented east-west and north-south. The east-west line is near to the Pierce Junction Salt Dome and travels ~9600 m along Old Spanish Trail Highway. The north-south line passes just to the east of the University of Houston and travels ~7500 m along the Spur 5 Bypass and doglegs through the neighborhood leading to the back of the George R. Brown Convention Center. The east-west line included 287 geophones and 203 shots, and the north-south line includeds 213 geophones and 164 shots. Shot spacing and geophone spacing is equal to 110 ft (33.5 m). Four Vibroseis trucks were used with a swept frequency source from 6–96 Hz. The unconsolidated near-surface sediments attenuate the signal energy due to the earth acting as a low pass filter. Thus, the total sweep length used was 8 s to insure the energy was strong enough to propagate into the subsurface (Liner, 1999). In the Houston area, the top sediments are clays and muds, and the high frequency part of Vibroseis energy was trapped in the near-surface section.

Seismic acquisition in the city has many obstacles including noise from traffic, engineering work, and trains. The advanced processing techniques used focus on shallow targets, but the first processing step is to remove noise from the raw data. The seismic signal is contaminated with considerable background noise due to the traffic and other environmental noise. To remove the noise, an automatic gain control (AGC) filter was used with a 500 ms window length and 0.1 scale factor before being correlated with the sweep. The signal to noise ratio was significantly improved by changing the AGC scale factor from 1 to 0.1 before the cross-correlation process. The spiking deconvolution filter was set with a 400 ms operator length and applied to the data. The raw record was then subtracted from the deconvolved record to remove background noise.

After the shot gather analysis, a 15/20–50/60 Hz Ormsby filter and 60 Hz notch filter were applied. Once these steps were completed a conventional workflow was applied that used normal move-out (NMO) velocity analysis, brute stack, and time migration (Table 1). The first arrival velocities were used in the time-depth conversion (Fig. 2). There are two horizons picked on both seismic profiles (Fig. 3). The green horizon is interpreted as the base of Evangeline Aquifer and the blue horizon is interpreted as the base of Jasper Aquifer based on local stratigraphy (Fig. 4).

Gravity Forward Modeling

The field gravity data used in this study is a 7600 m long line with 39 stations at 200 m intervals. The orientation of the 2D profile is in a southwest-northeast direction (azimuth of 18°) to the north across the salt dome, along Almeda Road (Fig. 1). The survey line crossing the Pierce Junction Salt Dome was acquired using a Scintrex CG–5 Autograv gravimeter. A Garmin GPS was used to record locations and measure distances (Coskun, 2014). The gravity processing included applying latitude, free-air, and Bouguer corrections to the data. The stratigraphic sequence of the west-east cross section of the Pierce Junction Salt Dome was modified based on Glass (1953) and Holzer and Bluntzer (1984). GEOSOFT Oasis Montaj software was used to calculate the forward model (Fig. 5).

RESULTS

Data from the three geophysical techniques have been used to map new faults and segments of a previously unknown fault system. Four new fault segments were mapped in this study (Fig. 1). Results of the LiDAR data include a high-resolution Digital Elevation Model (DEM) to identify active fault scarps. A hillshade map highlights the fault segment 2 near the medical center and the western part of a seismically-mapped fault segment 1. These fault scarps are small and typically have ~0.8 ft (~0.25 m) of displacement and dip towards the south (Fig. 1, fault segment 2). Regions of interest identified in the hillshade surfaces were further investigated during targeted fieldwork. This included field observations recorded during and after data acquisition that were used to ground truth the geophysical datasets. These surface manifestations show that surface deformation is both widespread and active in the regions targeted by LiDAR, seismic, and gravity data.

Results from the analysis of the seismic data include the identification of a fault that is near vertical at the intersection of our two seismic lines (Fig. 1, fault segment 1). A refraction method was used to obtain the average velocity for the near-surface sediments of around 5900 ft/s (~1800 m/s). In a noisy traffic area covered with unconsolidated sediment composed of clay, it is necessary to improve the signal to noise ratio. A novel processing strategy was designed and applied to the acquired data. In spite of the strong cultural noise observed in the data, processing techniques have partially overcome the adverse field conditions and allowed imaging of seismic reflections up to 1.4 s (two-way travel times) with a vertical resolution of ~10 m. The processed seismic lines clearly show a near-vertical fault at the cross point of the two profiles with a fault plane that dips towards the southeast with ~20 m displacement. Based on the average velocity the approximate depth of the base of the fault is at least ~3800 ft (~1160 m), and the maximum image depth is ~4100 ft (~1250 m). The north-south seismic profile shows the picked horizons dipping south toward the Gulf of Mexico.

The gravity Bouger anomaly caused by the Pierce Junction Salt Dome and its associated faults were modeled and two gravity variations on the northeast and southwest sides of the profile are considered in this interpretation as active faults (Fig. 1, fault segments 3 and 4). From a 2D seismic image located at the center of the salt dome, it was suggested that the cap rock and top of the salt are 205 m and 290 m below the present surface, respectively (Coskun, 2014).

DISCUSSION

The unconsolidated nature of shallow subsurface sediments in Houston allows rapid erosion to mask the fault movement such that only currently active faults have identifiable surface fault scarps. It is likely that the faults identified in the LiDAR and seismic data is active because of the observed surface defor-

Table 1. Seismic processing workflow.

Processing Steps	Description	Parameters
Create a project	Load raw un-correlated data	▪ Using VISTA software
Geometry setup	Geometry description for geophones and sources	▪ Source spacing~110 ft, Geophone Spacing~110 ft
Trace editing	Remove the dead traces	
Vibroseis correlation	Cross correlation with the sweep	▪ L1 norm equalization ▪ Length of Automatic Gain Control (AGC) window: 500 ms ▪ Output scale factor: 0.1 ▪ Sweep length: 8000 ms
Deconvolution	Surface consistent deconvolution	▪ Decon. type: spiking decon ▪ Operator length: 400 ms ▪ Pre-whitening: 1% ▪ Operator design window: entire trace
Subtract	Remove the background noise	▪ Deconvolved subtract the correlated
First arrival picking & mute		▪ Mute up to the first arrival time
Notch filter & band pass filter	Ormsby band pass	▪ 60 Hz Notch for power line noise ▪ 15/20-50/60 Hz band to improve SNR
Semblance velocity analysis	True surface Normal Move-Out (NMO)	▪ Stretch mute: 30% ▪ Velocity percent: 100%
Brute stack	Common Mid-Points (CMP) stack	▪ Stack option: 1/(N+1)
Time migration	2D finite difference migration	▪ Based on the NMO velocity model ▪ Aperture: 15 degree

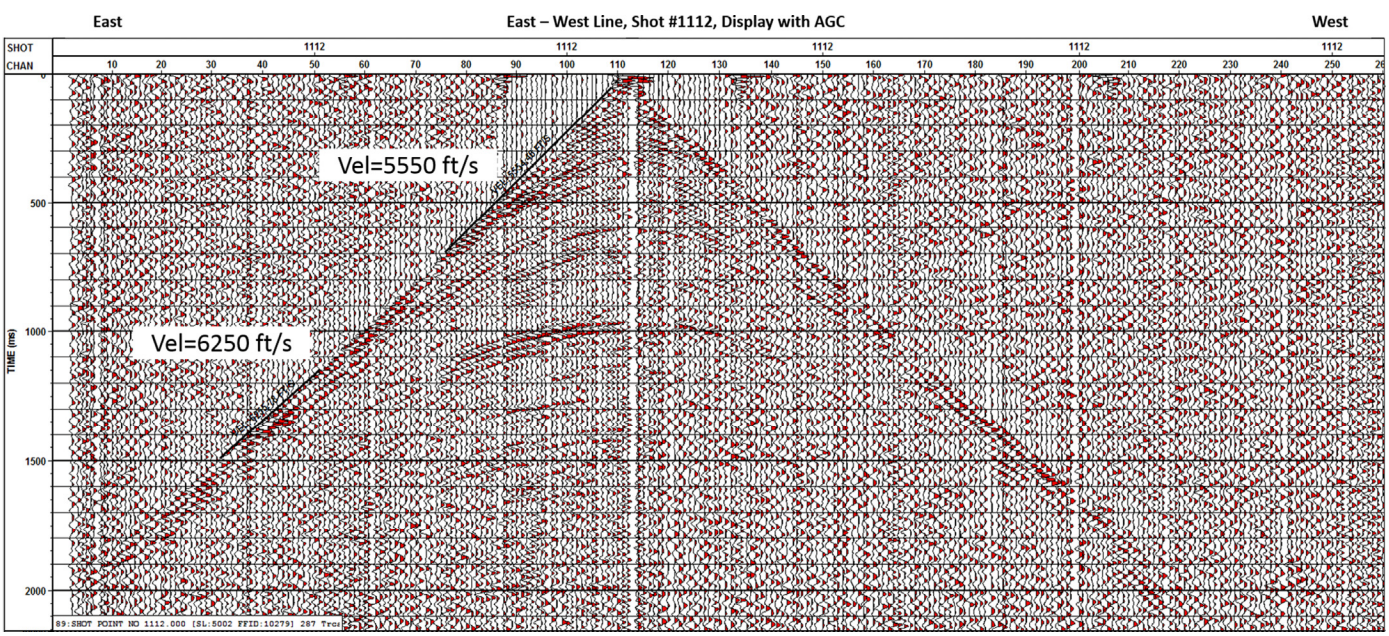

Figure 2. A two-dimensional velocity model calculated using the first arrival time. Based on these velocities, a time and depth relationship is established for time-depth conversion.

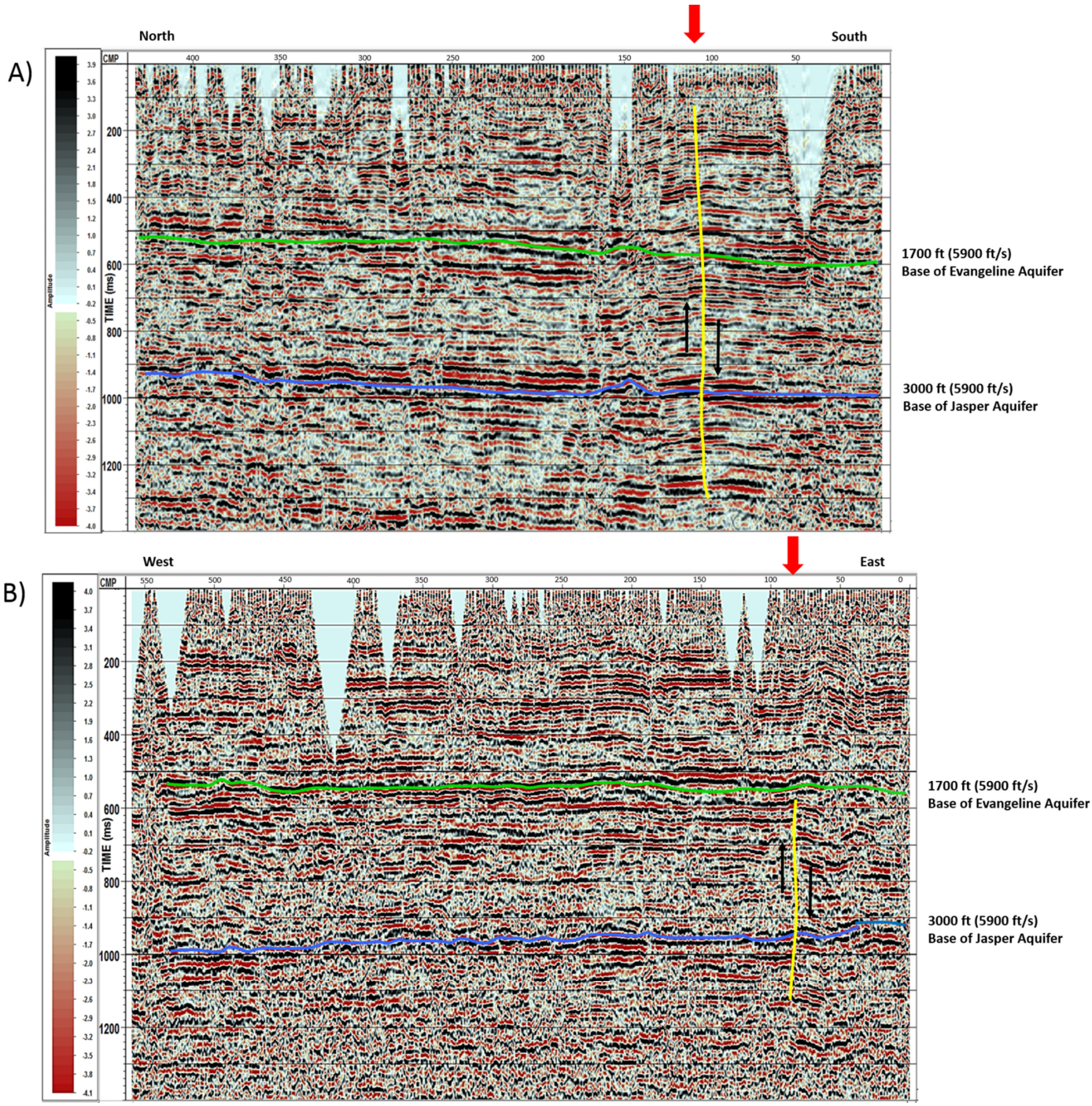

Figure 3. (A) 24,500 ft (~7500 m) long north-south time migrated section. (B) 31,500 ft (~9600 m) long east-west time migrated section. The depths are in two-way time (TWT). The seismic traces peak amplitude is shown in black and the trough in red. The horizons have been picked on the trough amplitude. The two horizons can be picked on both seismic profiles. Red arrows show the location where the two orthogonal profiles cross. The newly-identified fault segment 1 is shown by the yellow-colored line. The vertical resolution of the seismic profile is around 35 ft (~10 m). The displacement of the fault is around 70 ft (~20 m). The north-south seismic profile shows the picked horizons slightly dip to the south.

mation. Fault segment 1 identified in the seismic data occurs in a river valley where no surface deformation was observed presumably because pervasive erosion removed any scarp that would have be evidence of an active fault. The strike of the conjectured fault segment 1 plane follows the trend and dip direction of other mapped faults in Houston. This suggests that the newly recognized fault segment 1 is part of an existing regional fault and part of the gravity-driven regional fault population. The LiDAR data shows the location of surface deformation for a fault where recent erosion has not removed the scarp. Using this integrated dataset, we have found evidence for fault segment 2. Fault segments 3 and 4 mapped in the gravity profile have no surface scarp. This is likely because soft unconsolidated sediment cannot be fractured and it naturally infills due to surface erosion and deposition as long as the rate of offset along the underlying fault is minimal.

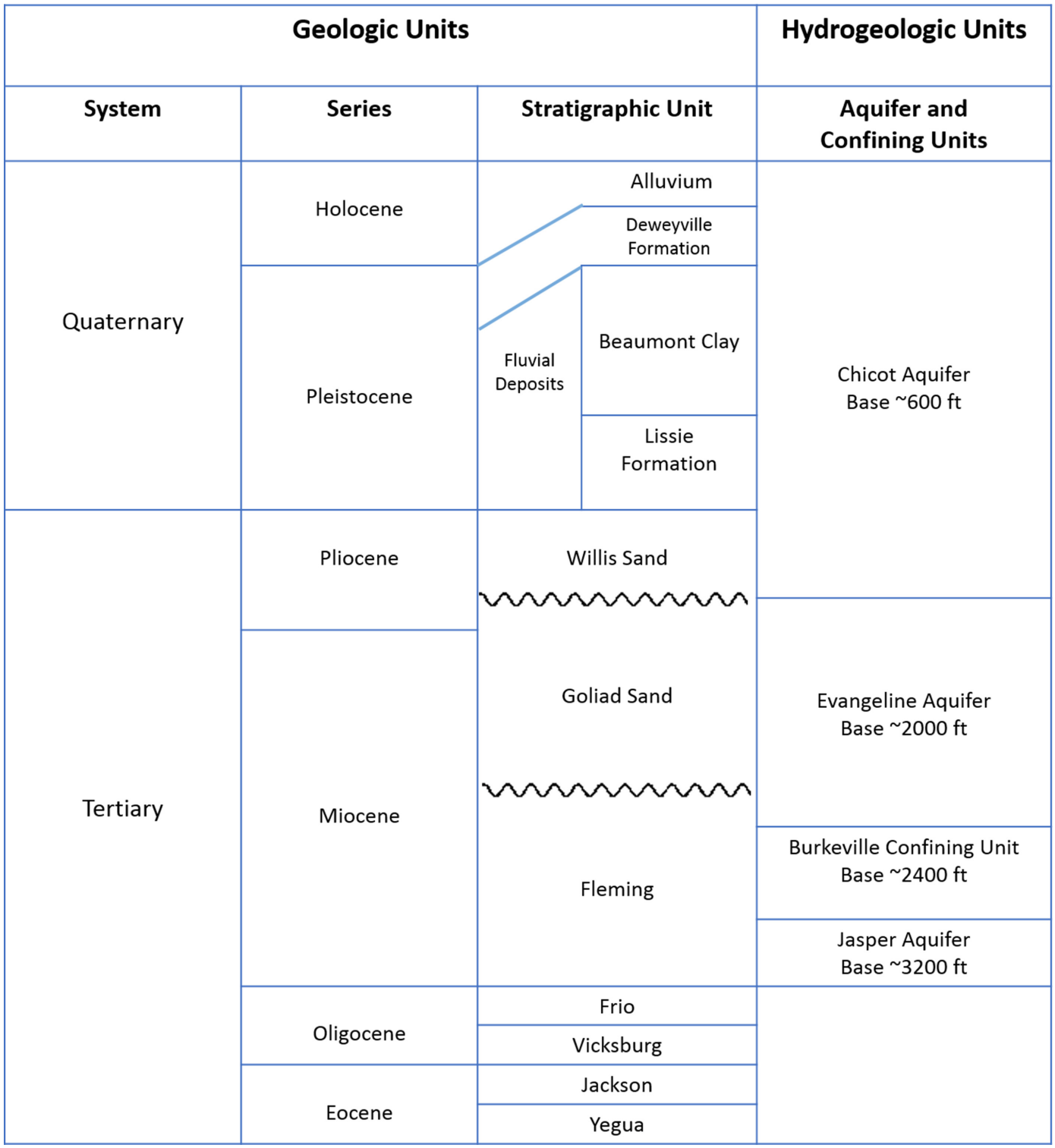

Figure 4. Generalized stratigraphy of the Eocene-Holocene (in part) series for southeastern Texas. The depths are based on a Gulf Coast hydrologic cross section from Baker (1979) and modified based on Baskin and Hulbert (2008).

Fluid withdrawal is a well-documented mechanism for subsidence in the Houston and Galveston region (White and Morton, 1997; White and Tremblay, 1995; Winslow and Doyel, 1954). There is general agreement that a relationship exists between fluid withdrawal and faulting (Castle and Youd, 1972; McClelland Engineers, 1966; Kreitler, 1976, 1977; Van Siclen, 1967). Fault creep and subsidence has stopped or slowed in the eastern part of Houston, where reductions in pumping of groundwater have allowed water levels to partially recover (Holzer and Gabrysch, 1987). Verbeek and Clanton (1981) expanded on the hypothesis that fluid withdrawal in the Houston metropolitan area has accelerated movement on preexisting faults. Groundwater extraction has triggered movement on more than 86 faults (Holzer and Galloway, 2005). Fluid withdrawal may accelerate displacement along the existing regional faults causing further fault propagation, including the newly-mapped fault segment 1.

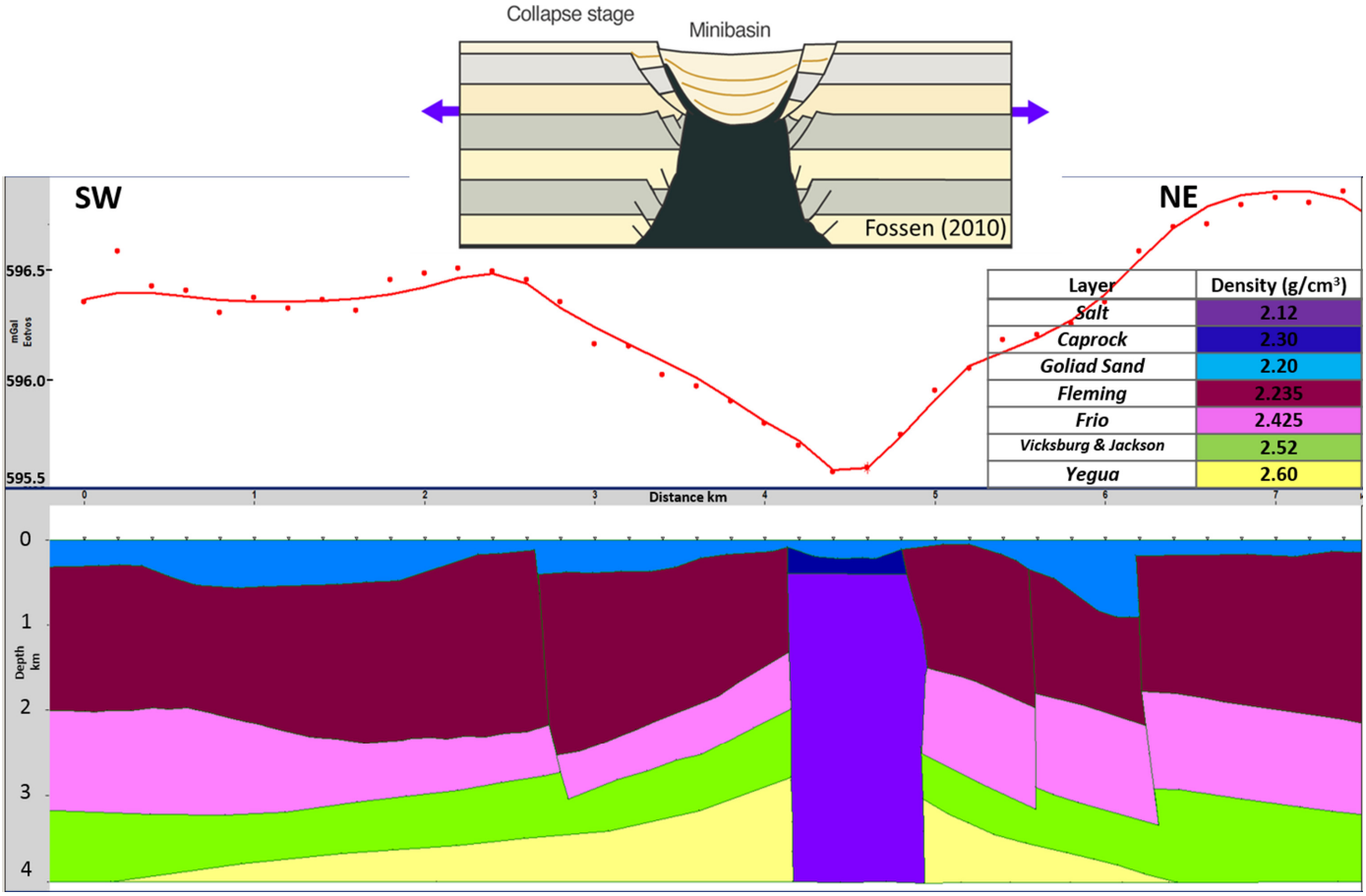

Figure 5. 7600 m long gravity profile cross Pierce Junction Salt Dome. Red dots and red line represent the observed and calculated gravity, respectively. Fault segments 3 and 4 were modeled based on the gravity data (Fossen, 2010).

Much of the surface deformation seen in the GPS rate variations (subsidence and especially uplift) in Houston cannot be explained only by fluid withdrawal of water and oil. The newly-mapped fault segments 2, 3, and 4 show the potential for deformation caused by salt withdrawal, associated with subsidence seen at and around the Pierce Junction Salt Dome based on GPS data. Elsewhere we see consistent subsidence rates off of the flanks of the salt domes but uplift east of this area (Fig. 1). The faults need continued monitoring and additional characterization to enable a fuller understanding of the fault mechanisms and to make a more thorough hazard assessment.

SUMMARY AND CONCLUSIONS

Data from the three geophysical techniques—seismic, LiDar, and gravity—have been used to map new fault segments. The four newly-mapped fault segments provide more detailed explanation for the surface deformation of the Pierce Junction, medical center area, and downtown Houston. The seismic lines resulted in newly-mapped fault segment 1. The 2D seismic profiles show the displacement of the fault is 70 ft (~20 m) (Fig. 3). By combining the previously-mapped fault and the bending of a creek, we interpreted that fault segment 1 is part of the gravity-driven regional fault population. The arc of the fault is shown in Fig. 1. The strike of the conjectured fault plane follows the trend and dip direction of other mapped faults in Houston. This may indicate that the newly recognized fault segment 1 is likely part of an existing regional fault zone. Fault segments 2, 3, and 4 are caused by salt withdrawal from the Pierce Junction Salt Dome. Regional seismic interpretation and modeling in the greater Houston metropolitan area will help to understand the mechanism of the deep-seated subsidence. The newly-mapped fault segments hold the potential to provide an assessment of surface deformation and improve future city planning and development. The addition of new faults to the existing Houston fault maps will lead to a broader understanding of neotectonics of Houston.

ACKNOWLEDGMENTS

We would like to thank Bob Van Nieuwenhuise for advice on the seismic data processing. We would also like to thank DAWSON Geophysical Company for acquiring the seismic data and Dr. Robert Stewart for allowing us to use the gravity data. We also thank Dr. Richard Engelkemeir, Dr. Barry Katz, and Dr. Greg Schoenborn for their very helpful reviews that significantly improved this paper.

REFERENCES CITED

Baker, E. T., 1979, Stratigraphic and hydrogeologic framework of part of the Coastal Plain of Texas: Texas Department of Water Resources Report 236, Austin, 32 p.

Baskin, J. A., and R. C. Hulbert, 2008, Revised biostratigraphy of the middle Miocene to earliest Pliocene Goliad Formation of South Texas: Gulf Coast Association of Geological Societies Transactions, v. 58, p. 93–101.

Castle, R., and T. Youd, 1972, Discussion: The Houston fault problem: Association of Engineering Geologists Bulletin, v. 9, p. 57–68.

Clanton, U. S., and E. R. Verbeek, 1981, Photographic portrait of active faults in the Houston metropolitan area, Texas, *in* E. M. Etter, ed., Houston area environmental geology: Surface faulting, ground subsidence, and hazard liability: Houston Geological Society, Texas, p. 70–113.

Coskun, S., 2014, 3–D Seismic survey design via modeling and reverse time migration: Pierce Junction Salt Dome, Texas: M.S. Thesis, University of Houston, Texas, 161 p.

Diegel, F., J. Karlo, D. Schuster, R. Shoup, and P. Tauvers, 1995, Cenozoic structural evolution and tectono-stratigraphic framework of the northern Gulf Coast continental margin, *in* M. P. A. Jackson, D. G. Roberts, and S. Snelson, eds., Salt tectonics: A global perspective: American Association of Petroleum Geologists Memoir 65, Tulsa, Oklahoma, p. 109–151.

Engelkemeir, R., S. D. Khan, and K. Burke, 2010, Surface deformation in Houston, Texas using GPS: Tectonophysics, v. 490, p. 47–54.

Engelkemeir, R. M., and S. D. Khan, 2008, Lidar mapping of faults in Houston, Texas, USA: Geosphere, v. 4, p. 170–182.

Ewing, T. E., and R. F. Lopez, 1991, Principal structural features, Gulf of Mexico Basin, *in* A. Salvador, ed., The geology of North America, v. J: The Gulf of Mexico Basin: Geological Society of America, Boulder, Colorado, Plate 2, scale 1:2,500,000, 1 sheet.

Fossen, H., 2010, Structural geology: Cambridge University Press, U.K., 463 p.

Geomap Company, 2015, <https://www.geomap.com> Accessed March 2015.

Glass, C., 1953, Pierce Junction Field: Harris County, Texas, *in* Guidebook, field trip routes, oil fields, geology: Houston Geological Society, Texas, p. 147–150.

Holzer, T. L., and R. L. Bluntzer, 1984, Land subsidence near oil and gas fields, Houston, Texas: Ground Water, v. 22, p. 450–459.

Holzer, T. L., and R. K. Gabrysch, 1987, Effect of water-level recoveries on fault creep, Houston, Texas: Groundwater, v. 25, p. 392–397.

Holzer, T. L., and D. L. Galloway, 2005, Impacts of land subsidence caused by withdrawal of underground fluids in the United States: Reviews in Engineering Geology, v. 16, p. 87–99.

Huang, Z., 2012, Multidisciplinary investigation of surface deformation above salt domes in Houston, Texas: M.S. Thesis, University of Houston, Texas, 106 p.

Jackson, M. P., and W. E. Galloway, 1984, Structural and depositional styles of Gulf Coast Tertiary continental margins: Application to hydrocarbon exploration: American Association of Petroleum Geologists Continuing Education Course Note Series 25, Tulsa, Oklahoma, 226 p.

Khan, S. D., Z. Huang, and A. Karacay, 2014, Study of ground subsidence in northwest Harris County using GPS, LiDAR, and InSAR techniques: Natural Hazards, v. 73, p. 1143–1173.

Khan, S. D., R. R. Stewart, M. Otoum, and L. Chang, 2013, A geophysical investigation of the active Hockley Fault System near Houston, Texas: Geophysics, v. 78, p. B177–B185.

Kreitler, C. W., 1976, Faulting and land subsidence from groundwater and hydrocarbon production, Houston-Galveston, Texas: Texas Bureau of Economic Geology Research Note 8, Austin, 22 p.

Kreitler, C. W., 1977, Fault control of subsidence, Houston, Texas: Groundwater, v. 15, p. 203–214.

Liner, C. L., 1999, Elements of 3-D seismology: Pennwell Books, Tulsa, Oklahoma, 608 p.

McClelland Engineers, 1966, Land-surface subsidence and surface faulting (appendix C), *in* Turner, Collie, and Braden, Inc., A comprehensive study of Houston's municipal water system: Report to the City of Houston, Texas, 50 p.

Peel, F., C. Travis, and J. Hossack, 1995, Genetic structural provinces and salt tectonics of the Cenozoic offshore US Gulf of Mexico: A preliminary analysis, *in* M. P. A. Jackson, D. G. Roberts, and S. Snelson, eds., Salt tectonics: A global perspective: American Association of Petroleum Geologists Memoir 65, Tulsa, Oklahoma, p. 153–175.

Rowan, M. G., M. P. Jackson, and B. D. Trudgill, 1999, Salt-related fault families and fault welds in the northern Gulf of Mexico: American Association of Petroleum Geologists Bulletin, v. 83, p. 1454–1484.

Saribudak, M., 2011, Geophysical mapping of the Hockley growth fault in northwest Houston, USA, and recent surface observations: The Leading Edge, v. 30, p. 172–180.

Saribudak, M., and B. Van Nieuwenhuise, 2006, Integrated geophysical studies over an active growth fault in Houston: The Leading Edge, v. 25, p. 332–334.

TNRIS (Texas Natural Resources Information System), 2015, <https://tnris.org/> Last accessed August 30, 2015.

Van Siclen, D. C., 1967, The Houston fault problem: American Institute of Professional Geologists, Texas Section: Third Annual Meeting Proceedings, p. 9–31.

Verbeek, E. R., 1979, Quaternary fault activity in Texas Gulf Coast: American Association of Petroleum Geologists Bulletin, v. 63, p. 545–545.

Verbeek, E. R., and U. S. Clanton, 1981, Historically active faults in the Houston metropolitan area, Texas, Houston area environmental geology, *in* E. M. Etter, ed., Houston area environmental geology: Surface faulting, ground subsidence, and hazard liability: Houston Geological Society, Texas, p. 28–68.

White, W. A., and R. A. Morton, 1997, Wetland losses related to fault movement and hydrocarbon production, southeastern Texas coast: Journal of Coastal Research, p. 1305–1320.

White, W. A., and T. A. Tremblay, 1995, Submergence of wetlands as a result of human-induced subsidence and faulting along the upper Texas Gulf Coast: Journal of Coastal Research, p. 788–807.

Winslow, A. G., and W. W. Doyel, 1954, Land-surface subsidence and its relation to the withdrawal of ground water in the Houston-Galveston region, Texas: Economic Geology, v. 49, p. 413–422.

Worrall, D. M., and S. Snelson, 1989, Evolution of the northern Gulf of Mexico, with emphasis on Cenozoic growth faulting and the role of salt, *in* A. W. Bally and A. R. Palmer, eds., The geology of North America, v. A : Geological Society of America, Boulder, Colorado, p. 97–138.

Wu, S., P. R. Vail, and C. Cramez, 1990, Allochthonous salt, structure and stratigraphy of the north-eastern Gulf of Mexico. Part I: Stratigraphy: Marine and Petroleum Geology, v. 7, p. 318–333.

Yu, J., G. Wang, T. J. Kearns, and L. Yang, 2014, Is there deep-seated subsidence in the Houston-Galveston area?: International Journal of Geophysics, v. 2014, Article 942834, 11 p.

View publication stats